ELSEVIER

Chemical Engineering Journal 87 (2002) 171–179

Chemical Engineering Journal

www.elsevier.com/locate/cej

A study of carbon dioxide absorption into aqueous monoethanolamine solution containing calcium nitrate in the gas–liquid reactive precipitation of calcium carbonate

M. Vučak [a,1], J. Perić [a,*], A. Žmikić [a], M.N. Pons [b]

[a] *Faculty of Chemical Technology, University of Split, Teslina 10/V, HR-21000 Split, Croatia*

[b] *Laboratoire des Sciences du Génie Chimique (CNRS-ENSIC-INPL), 1 rue Grandville BP 451, F-54001 Nancy Cedex, France*

Received 4 December 2000; received in revised form 30 August 2001; accepted 12 September 2001

Abstract

The influence of calcium nitrate on the process of carbon dioxide absorption in aqueous monoethanolamine (MEA) solution has been considered. The experimental data obtained under typical conditions used for the industrial precipitation of calcium carbonate has been used to determine the speciation in solution and the supersaturation profile in the bulk liquid by means of a specially developed algorithm as well as the kinetic regime of the absorption process in a pure aqueous solution and in the presence of calcium species at 30 °C using equilibrium and kinetic data from the literature. As expected, in pure MEA solution carbon dioxide reacts with MEA yielding ethanolammonium carbamate, whereas in the presence of calcium nitrate the process shifts towards $CaCO_3{}^0$ ion pair formation, resulting in a continuous increase of the supersaturation generated during the "induction period" of calcium carbonate precipitation. The proposed reaction mechanism is supported also by the precipitate morphology determined by SEM analysis.

Keywords: $CaCO_3$; Gas–liquid–solid (precipitation, crystallization); Carbonation; Carbon dioxide; MEA

1. Introduction

Alkanolamine solutions are frequently used for the removal of acid gases (carbon dioxide) from industrial and natural gas streams. Simultaneous absorption and the reactions between CO_2 and alkanolamine solutions have been studied extensively [1,2]. Versteeg et al. [3] provided an overview of some research work on this topic.

In aqueous solutions, CO_2 reacts with monoethanolamine (MEA) (RNH_2) yielding ethanolammonium carbamate according to the following overall reaction [4]:

$$CO_{2(g)} + 2RNH_{2(l)} \rightleftarrows RNH_{3(aq)}{}^{+} + RNHCOO_{(aq)}{}^{-} \quad (1)$$

The zwitterion reaction mechanism, originally proposed by Caplow [5] is generally accepted as the reaction mechanism [6,7]:

$$CO_{2(aq)} + RNH_{2(l)} \rightleftarrows RN^{+}H_2COO_{(aq)}{}^{-} \quad (2)$$

$$RN^{+}H_2COO_{(aq)}{}^{-} + RNH_{2(l)} \rightleftarrows RNH_{3(aq)}{}^{+} + RNHCOO_{(aq)}{}^{-} \quad (3)$$

The reverse inter-reaction (2), being slower, dictates the overall reaction rate (1). The overall reaction (1) can therefore be considered as an irreversible second-order reaction, i.e. a first-order reaction with regard to both CO_2 and amine, with the stoichiometric factor of 2, an equilibrium constant of the order of magnitude $10^5\,dm^3\,mol^{-1}$ [8], and $E_a = 41.2\,kJ\,mol^{-1}$ [4]. The effect of the reaction of CO_2 with the hydroxide ion is mainly negligible. Hikita et al. [8] stated that the correction of the rate constant for the overall reaction (1), due to the effect of the reaction with the hydroxide ion, does not exceed 4% [2,4,9,10].

In highly carbonated solutions with a carbonation ratio greater than 0.45 mol CO_2/mol MEA, carbamate hydrolysis reaction is usually assumed. The summary hydrolysis reaction can be shown as [11]:

$$RNHCOO_{(aq)}{}^{-} + H_2O_{(l)} \rightleftarrows HCO_{3(aq)}{}^{-} + RNH_{2(l)} \quad (4)$$

The reaction equilibrium constant (4) amounts to 0.025 mol dm^{-3} at 20 °C and 0.1 mol dm^{-3} at 50 °C [11].

The influence of calcium species on the aforementioned process has not been previously studied and is the objective of this paper.

In the case of production of calcium carbonate, the ethanolamine process is used for obtaining high-purity

* Corresponding author. Tel.: +385-21-385-633; fax: +385-21-384-964.
E-mail address: jelena.peric@ktf-split.hr (J. Perić).

[1] Now with Schaefer Kalk KG, Louise-Seher-Str. 6, D-65582 Diez, Germany.

1385-8947/02/$ – see front matter
PII: S1385-8947(01)00239-X

Nomenclature

A	Debye–Hückel constant (1)
Ca_T	total calcium concentration ($mol\,m^{-3}$)
CO_{2T}	total CO_2 dissolved ($mol\,m^{-3}$)
d	diameter of impeller (m)
D	diffusivity ($m^2\,s^{-1}$)
E	enhancement factor, defined by Eq. (14)
E_a	activation energy ($J\,mol^{-1}\,K^{-1}$)
E_i	enhancement factor, defined by Eq. (16)
I	ionic strength ($mol\,m^{-3}$)
k_L	liquid-phase mass transfer coefficient ($m\,s^{-1}$)
k_2	rate constant for reaction between CO_2 and amine molecules ($m^3\,mol^{-1}\,s^{-1}$)
K_b	chemical equilibrium constant defined in Table 1 ($mol\,m^{-3}$)
K_J	ion pair formation constant ($m^3\,mol^{-1}$)
K_k	chemical equilibrium constant defined in Table 1 ($m^3\,mol^{-1}$)
K_l	ion pair formation constant ($m^3\,mol^{-1}$)
K_L	chemical equilibrium constant defined in Table 1 ($m^3\,mol^{-1}$)
K_{sV}	solubility product of vaterite ($mol^2\,m^{-6}$)
K_w	ionic product of water ($mol^2\,m^{-6}$)
K_1	first ionization constant of carbonic acid ($mol\,m^{-3}$)
K_2	second ionization constant of carbonic acid ($mol\,m^{-3}$)
L	diameter of vessel (m)
M	parameter defined by Eq. (15)
N	speed of impeller (s^{-1})
$\bar{R}$	average rate of absorption, defined by Eq. (14) ($mol\,m^{-2}\,s^{-1}$)
Re	Reynolds number, defined by Eq. (13)
RNH_{2T}	total amine concentration ($mol\,m^{-3}$)
$[s]$	concentration of component s ($mol\,m^{-3}$)
S	supersaturation defined by Eq. (12), (1)
Sc	Schmidt number, defined by Eq. (13)
Sh	Sherwood number, defined by Eq. (13)
t	Celsius temperature (°C) or reaction time (s)
T	temperature (K)
v	rate of reaction (s^{-1})
z	charge number of ions (1), or stoichiometric coefficient (1)

Greek letters

α_t	reaction degree at time t (1)
γ_z	activity coefficient (1)
κ	conductivity ($S\,m^{-1}$)
μ	viscosity of liquid (Pa s)
ρ	density of liquid ($kg\,m^{-3}$)

precipitated calcium carbonate (PCC) of various crystal modifications, sizes and particle morphologies. The process is based on selective separation of the calcium component from a relatively impure source of calcium oxide in a solution of monoethanolammonium nitrate at controlled pH. Calcium carbonate obtained by carbonation of a solution thus prepared meets very high-purity criteria set for its application in the pharmaceutical, food-processing, cosmetics industry, etc. [12].

A study of such a semi-batch process, representing a complex heterogeneous reaction system with three phases involved—liquid, gaseous and solid—is of importance both from a theoretical and from an applied point of view. Determination of the process mechanism and kinetics, and the process conditions which would yield a product of desired properties, as well as quantifying their interdependencies, is of extreme importance, as it makes it possible to control, and thereby to manage, the process at optimal conditions.

The carbonation process, being the most important part of the ethanolamine process, results in precipitation, i.e. in formation of sparingly soluble calcium carbonate, induced by liquid-phase chemical reaction. The properties of the resulting product particles are determined by the process variables and their formation kinetics. The process involves gas–liquid mass transfer and chemical reaction, which proceed and generate the driving force for the crystallization, i.e. supersaturation, which is the fundamental parameter used in crystallization studies. Nucleation, subsequent crystal growth and different secondary processes (e.g. agglomeration, disruption, ageing, etc.) then follow at rates dependent on the level of supersaturation obtained. Although each of these basic processes has been studied in detail individually, the phenomenon of their combined activity has not been sufficiently researched because of its complexity.

In a previous work [13], special attention was therefore given to the aspect of crystal formation, especially focusing on morphological development during the process of carbonation. The present work aims to shed light on the speciation in solution and gas–liquid mass transfer phenomena.

2. Theory

2.1. Speciation and supersaturation

The experimentally obtained data is used to determine the changes in the concentration, or activities of the species present in the bulk solution and resulting supersaturation during the gas–liquid reactive precipitation of calcium carbonate at 30 °C. It is assumed that the liquid is well mixed, so that, it is uniform in composition, apart from the concentration gradients in the diffusion film close to the surface. The following species are taken into account: Ca^{2+}, OH^-, NO_3^-, RNH_2, RNH_3^+, $CaHCO_3^+$, HCO_3^-, CO_3^{2-}, $RNHCOO^-$, $CaCO_3^0$, H^+, $CO_{2(aq)}$ and $CaOH^+$. $CO_{2(aq)}$ has been defined as $CO_2^0 + H_2CO_3^0$ and pH =

Table 1
Equilibrium constants used in the computations

Species	Equilibrium constant (303 K)	Correction	Source
$CaOH^+$	$K_I = \frac{[CaOH^+]}{[Ca^{2+}][OH^-]} = 19.2579$	$\frac{K_I}{\gamma_2}$	[14]
$CaCO_3{}^0$	$K_J = \frac{[CaCO_3{}^0]}{[Ca^{2+}][CO_3{}^{2-}]} = 1867.5533$	$\frac{K_J}{\gamma_2^2}$	[15]
$CaHCO_3{}^+$	$K_K = \frac{[CaHCO_3{}^+]}{[Ca^{2+}][HCO_3{}^-]} = 13.6590$	$\frac{K_K}{\gamma_2}$	[15]
$RNH_3{}^+$	$K_b = \frac{[RNH_3{}^+][OH^-]}{[RNH_2]} = 3.322 \times 10^{-5}$	$K_b\gamma_1^2$	[1,16]; estimated
$HCO_3{}^-$	$K_1 = \frac{[H^+][HCO_3{}^-]}{[CO_2]} = 4.6975 \times 10^{-7}$	$K_1\gamma_1^2$	[15]
$CO_3{}^{2-}$	$K_2 = \frac{[H^+][CO_3{}^{2-}]}{[HCO_3{}^-]} = 5.1540 \times 10^{-11}$	$K_2\gamma_2$	[15]
$CaCO_3$(V) (vaterite)	$K_{sV} = [Ca^{2+}][CO_3{}^{2-}] = 1.1058 \times 10^{-8}$	$K_{sV}\gamma_2^2$	[15]
OH^-, H^+	$K_W = [H^+][OH^-] = 1.45 \times 10^{-14}$	$K_W\gamma_1^2$	[17]
$RNHCOO^-$	$K_L = \frac{[RNHCOO^-][RNH_3{}^+]}{[RNH_2]^2[CO_2]} = 21\,488.34$	$K_L\gamma_1^2$	[8,11]; estimated

$-\log([H^+]\gamma_1)$. Equilibrium constants, used in calculations, are shown in Table 1 where [] denotes molar concentration of species, and γ the activity coefficient of monovalent (γ_1) and divalent (γ_2) ions ($a = \gamma[c]$).

Additional equations necessary for the calculation are defined as follows.

Overall charge balance equation:

$$2[Ca^{2+}] + [RNH_3{}^+] + [CaHCO_3{}^+] + [CaOH^+] + [H^+] = [NO_3{}^-] + [OH^-] + [HCO_3{}^-] + 2[CO_3{}^{2-}] + [RNHCOO^-] \quad (5)$$

Overall mass balance equation for the total CO_2 dissolved (CO_{2T}):

$$CO_{2T} = [HCO_3{}^-] + [CO_3{}^{2-}] + [CaCO_3{}^0] + [CaHCO_3{}^+] + [RNHCOO^-] + [CO_{2(aq)}] + [CaCO_3(V)] \quad (6)$$

Overall mass balance equation for the measured total Ca concentration (Ca_T), assuming MEA does not form complexes with Ca [18] and $CaCO_3(V) = (Ca_T)_0 - (Ca_T)_t$:

$$Ca_T = [Ca^{2+}] + [CaCO_3{}^0] + [CaHCO_3{}^+] + [CaOH^+] \quad (7)$$

Overall mass balance equation for the total MEA (RNH_{2T}):

$$RNH_{2T} = [RNH_2] + [RNH_3{}^+] + [RNHCOO^-] \quad (8)$$

Ion activity coefficients are approximated based on the Davies equation [19]:

$$\log \gamma_z = -Az^2 \left(\frac{\sqrt{I}}{1+\sqrt{I}} - 0.3I \right) \quad (9)$$

where γ_z is the activity coefficient for ion with charge z and A the Debye–Hückel constant obtained by means of the interpolation formula [20]:

$$A = 0.492 + 0.00063t + 0.0000054t^2 \quad (10)$$

where t is the temperature (in °C).

The correction for the activity coefficient of the particular ionic species is neglected because of other uncertainties, which might introduce greater errors. This is probably a sufficiently close approximation for present purposes.

The ionic strength of the solution is obtained by means of the expression

$$I = 2[Ca^{2+}] + \tfrac{1}{2}[OH^-] + \tfrac{1}{2}[NO_3{}^-] + \tfrac{1}{2}[RNH_3{}^+] + \tfrac{1}{2}[CaHCO_3{}^+] + \tfrac{1}{2}[HCO_3{}^-] + 2[CO_3{}^{2-}] + \tfrac{1}{2}[RNHCOO^-] + \tfrac{1}{2}[CaOH^+] + \tfrac{1}{2}[H^+] \quad (11)$$

The supersaturation is finally obtained by inserting the data in the following equation:

$$S = \sqrt{\frac{[Ca^{2+}][CO_3{}^{2-}]\gamma_2^2}{K_{sV}}} \quad (12)$$

The system of equations is solved by means of a specially developed FORTRAN 90 program, which can be described by the following algorithm.

Algorithm

Part I

1. Initialization of equilibrium constants.
2. Initialization of the ionic strength.
3. Correction of the equilibrium constants for ionic strength.
4. Minimize the difference between experimental and estimated total CO_{2T}, given the experimental values of pH, MEA, total CO_{2T}, nitrate and calcium concentrations (see Part II).

5. Updating of the ionic strength.
6. If the ionic strength difference is larger than a preset value, go back to Step 3.
7. Else, end of the calculation.

Part II

The monovariable minimization is performed based on the Golden Section method within a specified interval. The objective function to be minimized is calculated as follows:

1. For a given value of $CO_{2(aq)}$.
2. Calculation of the various concentrations (H^+, OH^-, RNH_2, etc., see Eqs. (5)–(8)).
3. Calculation of a new value of total CO_{2T}.
4. Calculation of the objective function, i.e. relative error between the experimental total CO_{2T} concentration and the value estimated at Step 4 of Part I.
5. If the objective function is larger than a preset value, the Golden Section algorithm selects a new value for $CO_{2(aq)}$ and goes back to Step 2.
6. Else, the minimization is stopped and the program goes back to Step 5 of Part I.

Further details on the Golden Section method can be found in Ref. [21].

2.2. Gas–liquid mass transfer phenomena

Gas–liquid mass transfer phenomena determine the supersaturation generated by chemical reaction and its spatial distribution in the liquid-phase. It is therefore essential to predict its effect on the gas–liquid precipitation system studied. In order to define the kinetic regime of the absorption process under the specified operating conditions, the data on solubility and diffusivity in the aqueous MEA solution used, are needed. The physicochemical quantities are calculated applying the "N_2O analogy" as summarized by Versteeg et al. [3], and are presented in Table 2.

The mass transfer coefficient k_L at the gas–liquid interface is determined by the correlation [22]:

$$Sh = 0.322 Re^{0.7} Sc^{1/3} \tag{13}$$

where $Sh = k_L L/D_{CO_2}$, $Re = d^2 N\rho/\mu$ and $Sc = \mu/\rho D_{CO_2}$.

The kinetic regime of the absorption into agitated liquid, where the gas was blown through the liquid as a stream of bubbles, is estimated using an approximate set of solutions relating to the film model [23]. The second-order reaction of CO_2 into pure MEA solution is treated as though it was irreversible:

$$\frac{\bar{R}}{k_L[CO_2]} = E = \frac{\sqrt{M(E_i - E)/(E_i - 1)}}{\tanh\sqrt{M(E_i - E)/(E_i - 1)}} \tag{14}$$

where

$$M = \frac{D_{CO_2} k_2 [MEA]}{k_L^2} \tag{15}$$

$$E_i = 1 + \frac{D_{MEA}[MEA]}{z D_{CO_2}[CO_2]} \tag{16}$$

where E is the enhancement factor, i.e. the factor by which the rate of absorption is increased by the reaction and E_i the enhancement factor corresponding to instantaneous reaction, $\bar{R}$ the average rate of absorption over contact time, z the number of moles of reactant reacting with each mole of CO_2, $[CO_2]$ the concentration of dissolved CO_2 at interface in equilibrium with gas at interface, [MEA] the concentration of MEA in the bulk of liquid and k_2 the second-order rate constant for reaction of CO_2 with MEA.

The reaction rate v is expressed as a differential change [24]:

$$v_i = \left(\frac{d\alpha}{dt}\right)_i \tag{17}$$

which represents a function of reaction degree α_{Ca} and time t.

3. Experimental set-up

The absorption of carbon dioxide by aqueous MEA solution containing calcium nitrate is of major industrial importance, particularly in connection with the manufacture

Table 2
Calculated values of physicochemical constants at 303 K used in the computations

Parameter	Value	Source
ρ (kg m^{-3})	997.78	Present work applying "N_2O analogy"
μ (Pa s)	0.924×10^{-3}	Present work applying "N_2O analogy"
D_{CO_2} (m^2 s^{-1})	1.943×10^{-9}	Present work applying "N_2O analogy"
D_{MEA} (m^2 s^{-1})	1.122×10^{-9}	Present work applying "N_2O analogy"
m_{CO_2}	0.728	Present work applying "N_2O analogy"
k_L (m s^{-1})	4.5×10^{-5}	Present work using Eq. (13)
k_2 (m^3 mol^{-1} s^{-1})	10.2	[11]
$\sqrt{M}$	99	Present work using Eq. (15)
E_i	32	Present work using Eq. (16)
E	27	Present work, estimated
$\bar{R}$ (mol m^{-2} s^{-1})	0.0114	Present work using Eq. (14)

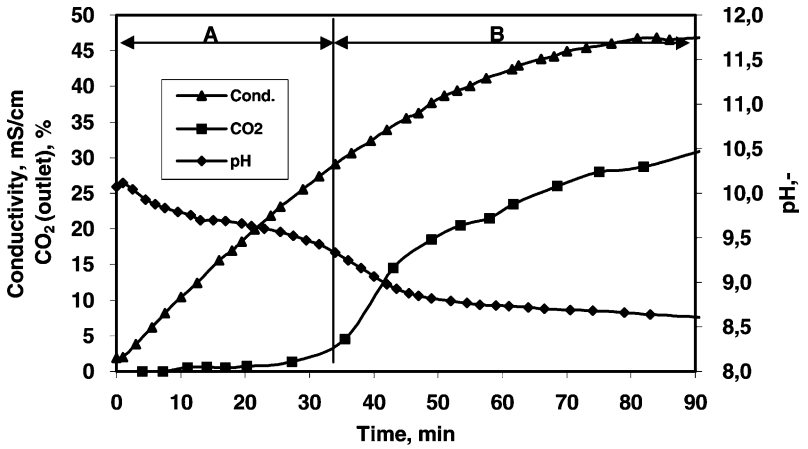

Fig. 1. Absorption of CO_2 in a pure aqueous solution of MEA.

of PCC. Therefore, the precipitation experiments were conducted under typical conditions used for the production of calcium carbonate. The carbonation (32.2% CO_2 in air) of freshly prepared calcium nitrate and MEA solution ($c_{Ca} = 0.5\,mol\,dm^{-3}$; $c_{HNO_3} = c_{MEA} = 1\,mol\,dm^{-3}$) was carried out in a 1 dm^3 L–S–G reactor made of stainless steel at 30 °C. The reactor was fitted with four vertical baffle plates and a six-blade turbine type impeller ensuring complete mixing. Freshly prepared solution reacted with the gas mixture, which was introduced from the bottom of the reactor. The mean pH and electrical conductivity of the solution were continuously recorded. CO_2 concentration at the contactor outlet was monitored by gas chromatography (Catharometer, Delsi Instruments Di7000). For liquid- and solid-phase analyses, the slurry was withdrawn from the precipitator by syringe, and immediately filtered through 0.2 μm Sartorius cellulose nitrate membranes with the help of syringe holders. The known amount of filtrate was diluted with a precise volume of dilute hydrochloric acid to prevent further precipitation and analyzed for total calcium by atomic absorption (Varian SpectrAA-20). The precipitate crystals were observed by scanning electron microscopy (SEM). The experimental set-up and procedure were identical to those described in detail previously [13].

4. Results and discussion

In order to analyze and to predict the overall process of the gas–liquid precipitation of calcium carbonate, a comparison between the carbonation of a pure MEA solution (control experiment) and a solution containing calcium species has been carried out.

4.1. Carbonation of a pure MEA solution

Time courses of different measured parameters during the process of CO_2 absorption obtained under the specified experimental conditions in a pure 1 M aqueous solution of MEA are shown in Fig. 1. The calculated concentration profiles for our system are shown in Fig. 2. Although, some of the parameters used for solving the relevant equilibrium equations had to be estimated, especially K_b and K_L, the calculated liquid compositions are probably sufficiently accurate to explain the experimental observations. This experiment is in agreement with theoretical predictions and with literature data [2–11].

The estimated values of the kinetic parameters presented in Table 2 indicate that the absorption takes place under conditions where the reactant is depleted near the surface, but the reaction is not fast enough to be treated as instantaneous.

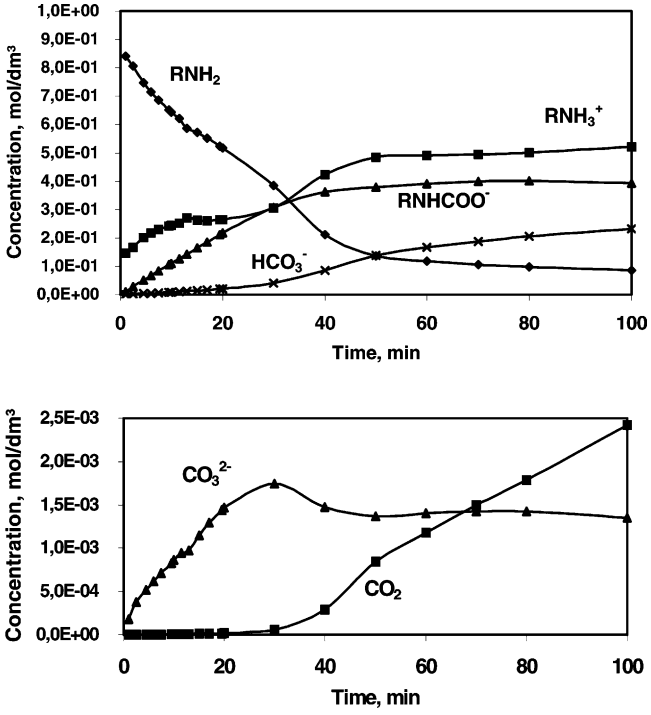

Fig. 2. Concentration profiles in the liquid.

Moreover, the absorption is almost entirely diffusion controlled. Therefore, the description of the phenomenon taking place is very complex, due to the nonlinearity of the expressions for the reaction kinetics and will be not considered in this work.

4.2. Carbonation in the presence of calcium nitrate

For the CO_2–MEA–$Ca(NO_3)_2$ system, the CO_2 absorption, i.e. precipitation of PCC, takes place in a solution of calcium nitrate and MEA, prepared by dissolving CaO in an equimolar solution of nitric acid and MEA. Preparation of the solution can be shown by the following reactions:

$$RNH_{2(l)} + H_{(aq)}{}^{+} + NO_{3(aq)}{}^{-} \rightleftarrows RNH_{3(aq)}{}^{+} + NO_{3(aq)}{}^{-} \quad (18)$$

$$2RNH_{3(aq)}{}^{+} + 2NO_{3(aq)}{}^{-} + CaO_{(s)} \rightleftarrows Ca_{(aq)}{}^{2+} + 2RNH_{2(l)} + 2NO_{3(aq)}{}^{-} + H_2O_{(l)} \quad (19)$$

The solution prepared is thus characterized by the high ionic strength of the solution ($0.5\,mol\,dm^{-3}\ Ca^{2+}$, $1\,mol\,dm^{-3}\ NO_3{}^{-}$) and a high pH (pH 11.4–12.2) due to hydrolysis of MEA:

$$RNH_{2(l)} + H_2O_{(l)} \rightleftarrows RNH_{3(aq)}{}^{+} + OH_{(aq)}{}^{-} \quad (20)$$

During the carbonation process, concentrations of individual species, especially Ca^{2+} and OH^{-} ions, change, and therefore the process was traced by measuring different parameters: Ca concentration, electric conductivity (hereafter, conductivity), CO_2 concentration in the outgoing gas and pH. The characteristic changes in parameters monitored are shown for the case of carbonation in the presence of calcium nitrate at 30 °C in Fig. 3. The time course of the liquid compositions and supersaturation are shown in Fig. 4.

According to the changes in the above parameters, the curves can be divided into three areas, A–C, as shown in Fig. 3. Analysis of parameters measured during the process, and comparison of the results with the data obtained for chemical absorption of CO_2 in a pure aqueous solution of MEA, suggest the following process mechanism.

Area A is characterized by a constant observed rate of absorption of CO_2 (Fig. 5) and constant concentration of Ca ($\alpha_{Ca} = 0$), which indicates the "induction period" of calcium carbonate precipitation. The solution displayed no turbidity in this area. The low concentration of CO_2 in the outgoing gas, i.e. the increase in the total CO_2 dissolved in the solution (α_{CO_2}), a drop in the pH value, and a slight increase in conductivity, can be mainly attributed to chemical absorption of CO_2 and to the reaction of $CaCO_3{}^{0}$ ion pair formation:

$$CO_{2(g)} \rightleftarrows CO_{2(aq)} \quad (21)$$

$$CO_{2(aq)} + OH_{(aq)}{}^{-} \rightleftarrows HCO_{3(aq)}{}^{-} \quad (22)$$

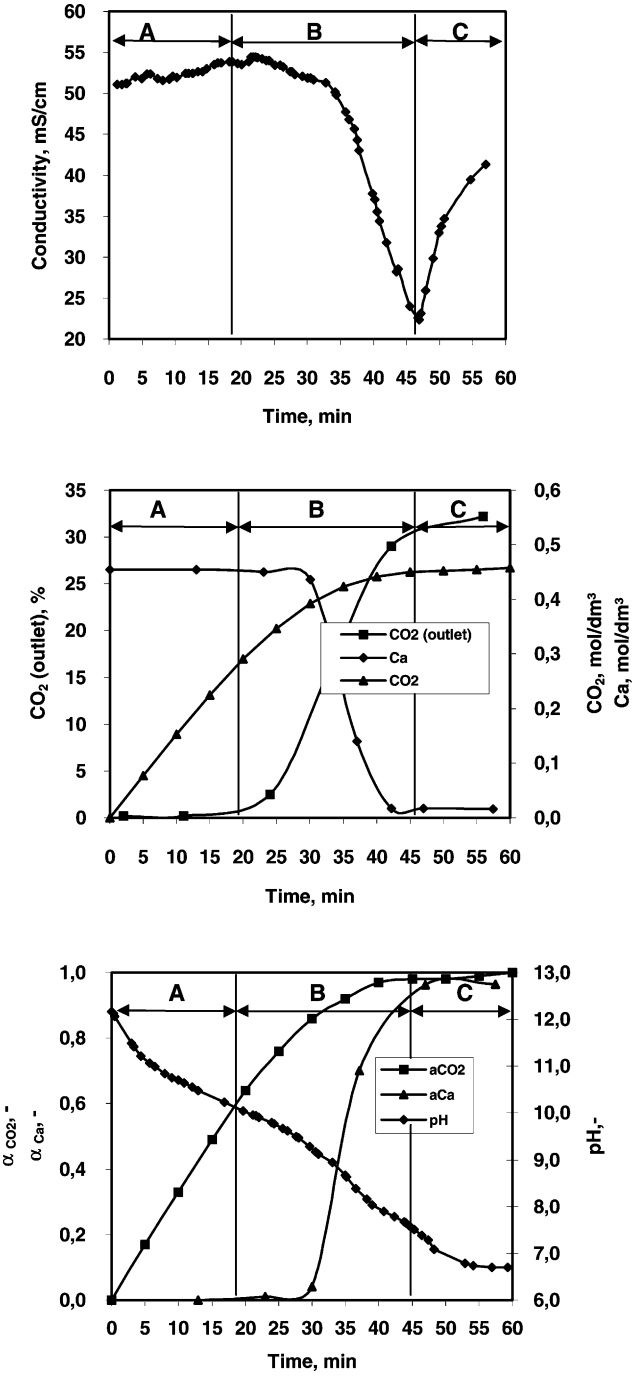

Fig. 3. Typical time course of the process of carbonation.

$$HCO_{3(aq)}{}^{-} + OH_{(aq)}{}^{-} \rightleftarrows CO_{3(aq)}{}^{2-} + H_2O_{(l)} \quad (23)$$

$$Ca_{(aq)}{}^{2+} + CO_{3(aq)}{}^{2-} \rightleftarrows CaCO_{3(aq)}{}^{0} \quad (24)$$

where $CaCO_3{}^{0}$ denotes an ion pair being produced by the action of Coulombic forces only. This is unambiguous evidence that in the presence of calcium nitrate, carbon dioxide will be progressively converted to the above-mentioned ion pair and elucidates on the reason for an "induction period" for calcium carbonate precipitation. This obviously

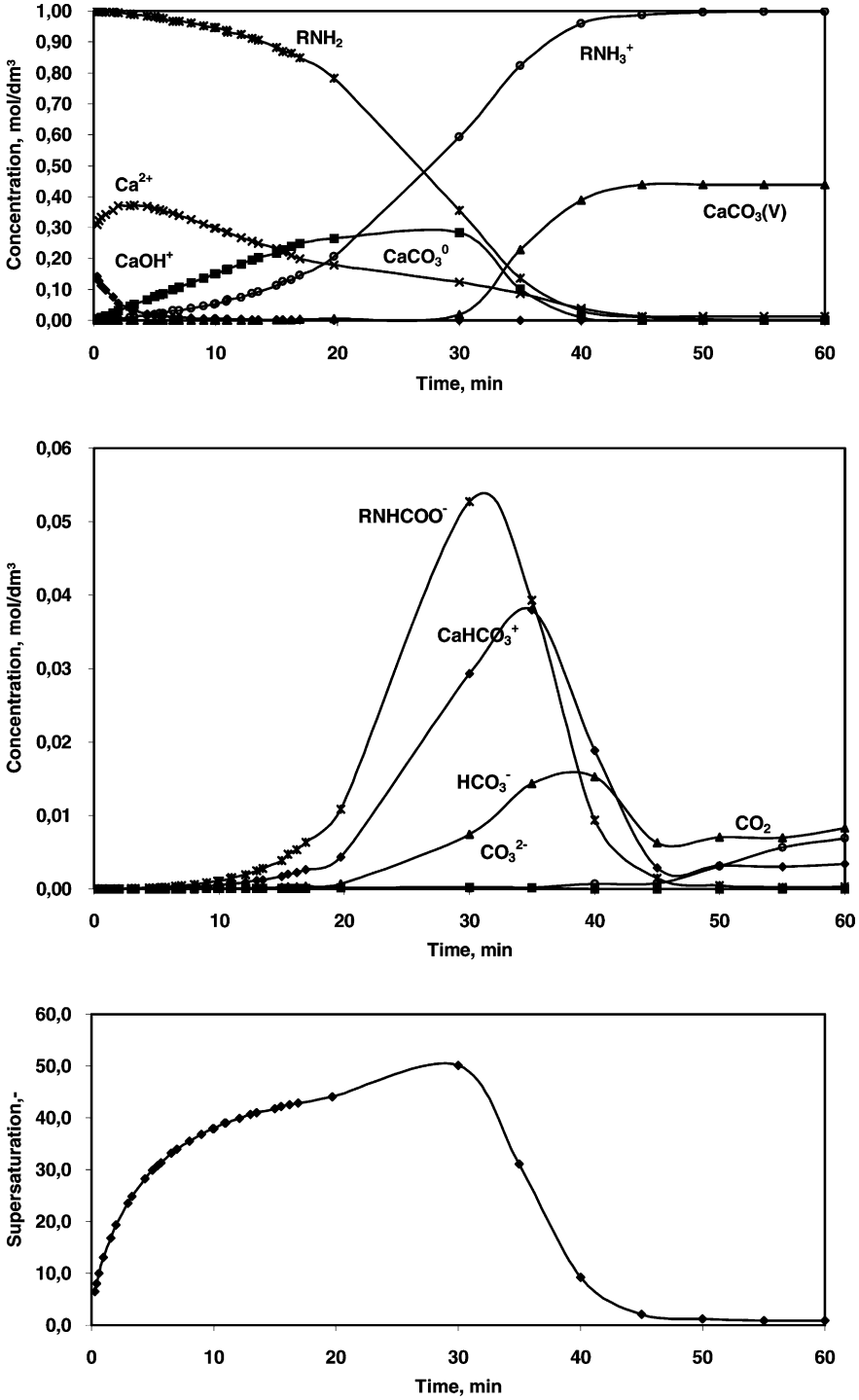

Fig. 4. Liquid compositions and the supersaturation profile for the process of carbonation.

enables the process of precipitation to be conducted in such a manner that the concentrations of constituent species reach critical supersaturation (Fig. 4), resulting in a short single burst of nuclei. Such initially formed, tiny dispersed solids coagulate into larger sponge-like vaterite spheres (Fig. 6), demonstrating the aggregation mechanism of particle growth [13,25].

A gradual decrease in the Ca concentration, in pH and conductivity, with further increase in the CO_2 concentration in the solution in the first part of the *Area B*, and an abrupt change in the Ca concentration with a negligible increase in the CO_2 concentration in the second part of the Area B, are ascribed to the increasing effect of the calcium carbonate precipitation reaction (25) and the contributions of different

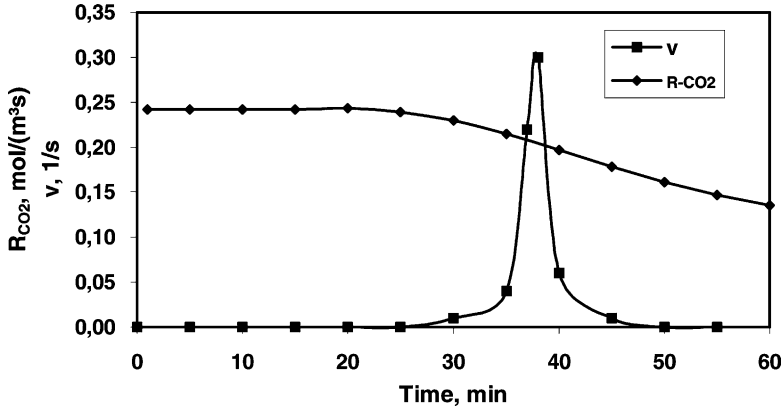

Fig. 5. Observed absorption rate of CO_2 and rate of precipitation process vs. time.

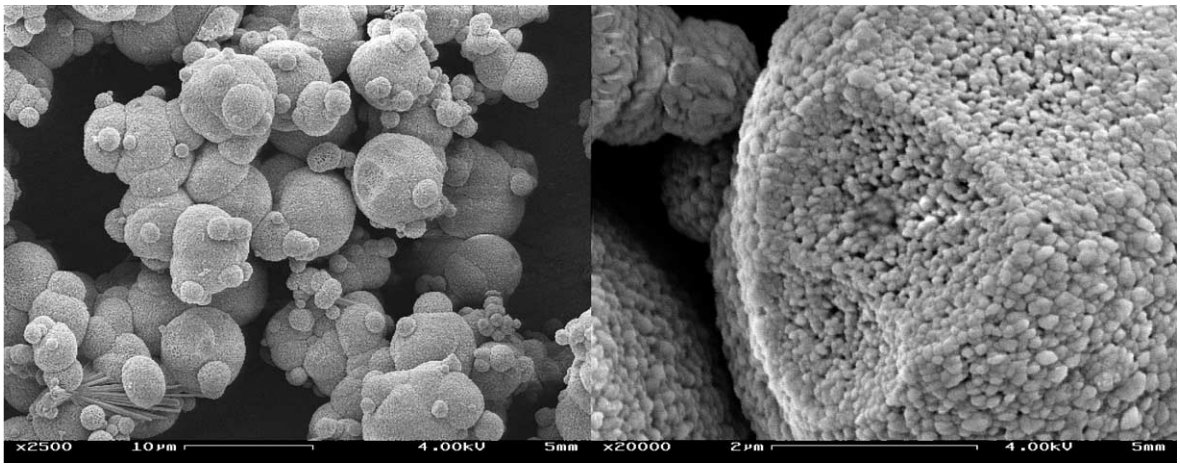

Fig. 6. Scanning electron micrographs of the vaterite spheres obtained by the process of carbonation.

secondary reactions with water, e.g. (26) or hydrolysis of carbamate (4):

$$Ca_{(aq)}{}^{2+} + CO_{3(aq)}{}^{2-} \rightleftarrows CaCO_{3(s)} \quad (25)$$

$$CO_{2(aq)} + H_2O_{(l)} \rightleftarrows HCO_{3(aq)}{}^{-} + H_{(aq)}{}^{+} \quad (26)$$

In the second part of Area B, the precipitation takes place at the maximum rate (Fig. 5) leading to the occurrence of agglomeration, which soon stops [13]. This suggests that the agglomeration is due to a low electric repulsion force, which in the case of high electric charge on the crystal surface, prevents the crystals from aggregating. A drop in the conductivity/Ca concentration to the lowest value, denotes the end of precipitation and corresponds to the equivalent point of calcium carbonate.

The increase in conductivity, and a slight drop in the pH value in the initial part of *Area C*, are caused mainly by the formation of $HCO_3{}^-$ and $CO_{2(aq)}$. The composition of the final solution, especially after CO_2 stripping, corresponds to the initial "equimolar" solution of ethanolammonium nitrate of higher conductivity ($\sim$70 mS cm^{-1}). This sudden increase in conductivity is the cause of the asymmetry of the κ–t curves.

The reaction mechanism assumed indicates extreme complexity of the carbonation process. The process includes gaseous, liquid and solid phases. The gaseous reactant absorbs in the solution in which, after a series of chemical reactions, sparingly soluble salt precipitates, governed by crystallization kinetics (nucleation, crystal growth rate and secondary processes). The process can be shown by the following overall reaction:

$$CO_{2(g)} + 2RNH_{2(l)} + Ca_{(aq)}{}^{2+} + H_2O_{(l)} \rightleftarrows 2RNH_{3(aq)}{}^{+} + CaCO_{3(s)} \quad (27)$$

5. Conclusions

The influence of calcium species on the reaction between CO_2 and MEA in the gas–liquid reactive precipitation of calcium carbonate has been investigated. Analysis of parameters measured during the process, and comparison of results

with data obtained for chemical absorption of CO_2 in a pure aqueous solution of MEA, where CO_2 reacts with MEA yielding ethanolammonium carbamate, indicate a very complex mechanism for the process. In the presence of calcium species, the reaction of CO_2 with hydroxide ions becomes significant, and the process shifts toward $CaCO_3{}^0$ ion pair formation, influencing the CO_2 absorption directly.

The induction period of calcium carbonate precipitation, marked by a constant observed rate period of absorption of CO_2 and an increase in supersaturation, can be ascribed to the chemical absorption of CO_2, i.e. to chemical speciation of complexes.

The preliminary calculations of gas–liquid mass transfer phenomena indicate that absorption under specified experimental conditions takes place under mass transfer limitations, rather than in the kinetically controlled regime. The effect of the reaction on the rate of absorption can, therefore, be evaluated only by rather complex calculations.

Acknowledgements

Part of this work was made possible by a grant awarded by the French Government to one of the authors.

References

[1] R.J. Littel, Selective carbonyl sulfide removal in acid gas treating processes, Ph.D. Thesis, University of Twente Enschede, The Netherlands, 1991.
[2] G.F. Versteeg, W.P.M. van Swaaij, On the kinetics between CO_2 and alkanolamines both in aqueous and non-aqueous solutions. I. Primary and secondary amines, Chem. Eng. Sci. 43 (1988) 573–585.
[3] G.F. Versteeg, L.A.J. van Dijck, W.P.M. van Swaaij, On the kinetics between CO_2 and alkanolamines both in aqueous and non-aqueous solutions: an overview, Chem. Eng. Commun. 144 (1996) 113–158.
[4] P.M.M. Blauwhoff, G.F. Versteeg, W.P.M. van Swaaij, A study on the reaction between CO_2 and alkanolamines in aqueous solutions, Chem. Eng. Sci. 39 (1984) 207–225.
[5] M. Caplow, Kinetics of carbamate formation and breakdown, J. Am. Chem. Soc. 90 (1968) 6795–6803.
[6] R.J. Littel, G.F. Versteeg, W.M.P. van Swaaij, Kinetics of CO_2 with primary and secondary amines in aqueous solutions. I. Zwitterion deprotonation kinetics for DEA and DIPA in aqueous blends of alkanolamines, Chem. Eng. Sci. 47 (1992) 2027–2035.
[7] R.J. Littel, G.F. Versteeg, W.P.M. van Swaaij, Kinetics of CO_2 with primary and secondary amines in aqueous solutions. II. Influence of temperature on zwitterion formation and deprotonation rates, Chem. Eng. Sci. 47 (1992) 2037–2045.
[8] H. Hikita, A. Asai, H. Ishikawa, M. Honda, The kinetics of reactions of carbon dioxide with monoethanolamine, diethanolamine and triethanolamine by rapid mixing method, Chem. Eng. J. 13 (1977) 7–12.
[9] B.R.W. Pinsent, L. Pearson, F.J.W. Roughton, The kinetics of combination of carbon dioxide with ammonia, Trans. Faraday Soc. 52 (1956) 1594–1598.
[10] G.F. Versteeg, J.A.M. Kuipers, F.P.H. van Beckum, W.P.M. van Swaaij, Mass transfer with complex reversible chemical reactions. I. Single reversible chemical reaction, Chem. Eng. Sci. 44 (1989) 2295–2310.
[11] P.V. Danckwerts, M.M. Sharma, The absorption of carbon dioxide into solutions of alkalis and amines, Chem. Engr. October (1966) CE244–CE280.
[12] M. Vučak, A study of the carbonation process with the quantification of calcium carbonate crystal shapes, Ph.D. Thesis, University of Split, Croatia, 1996.
[13] M. Vučak, J. Perić, M.N. Pons, S. Chanel, Morphological development in calcium carbonate precipitation by ethanolamine process, Powder Technol. 191 (1999) 1–6.
[14] L.D. Benefield, J.F. Judkins, B.L. Weand, Process Chemistry for Water and Wastewater Treatment, Prentice-Hall, London, 1982.
[15] L.N. Plummer, E. Busenberg, The solubilities of calcite, aragonite and vaterite in CO_2–H_2O solutions between 0 and 90 °C, for the system $CaCO_3$–CO_2–H_2O, Geochim. Cosmochim. Acta 46 (1982) 1011–1040.
[16] R.C. Weast, Handbook of Chemistry and Physics, 56th Edition, CRC Press, Cleveland, OH, 1975.
[17] F.H. Sweeton, R.E. Mesmer, C.F. Baes, Acidity measurements at elevated temperatures. VII. Dissociation of water, J. Solution Chem. 3 (1974) 191–214.
[18] L. Meites, Handbook of Analytical Chemistry, 1st Edition, McGraw-Hill, New York, 1963.
[19] C.W. Davies, Ion Association, Butterworths, London, 1962.
[20] R.A. Robinson, R.H. Stokes, Electrolyte Solutions, 2nd Edition, Butterworths, London, 1959.
[21] W.H. Ray, J. Szekely, Process Optimization, Wiley, New York, 1973.
[22] H. Hikita, H. Ishikawa, Physical absorption in agitated vessels with a flat gas–liquid interface, Bull. Univ. Osaka Prefect. A 18 (1969) 427–437.
[23] P.V. Danckwerts, Gas–Liquid Reactions, McGraw-Hill, New York, 1970.
[24] J. Perić, M. Vučak, R. Krstulović, Lj. Brečević, D. Kralj, Phase transformation of calcium carbonate polymorphs, Thermochim. Acta 277 (1996) 175–186.
[25] M. Vučak, M.N. Pons, J. Perić, H. Vivier, Effect of precipitation conditions on the morphology of calcium carbonate: quantification of crystal shapes using image analysis, Powder Technol. 97 (1998) 1–5.